Internal Report ITeSRE/CNR 273/2000

April 2000

A PRELIMINARY ANALYSIS OF IN-FLIGHT MAIN BEAM RECONSTRUCTION THROUGH EXTERNAL PLANETS FOR PLANCK-LFI

C. Burigana[1], P. Natoli[2], N. Vittorio[2],
N. Mandolesi[1] and M. Bersanelli[3]

[1]*Istituto TeSRE/CNR, via P. Gobetti 101, I-40129 Bologna, Italy*
[2]*Dipartimento di Fisica, Università di Roma "Tor Vergata", via della Ricerca Scientifica 1, I-00133, Roma, Italy*
[3]*Dipartimento di Fisica, Università di Milano, and IFC/CNR via Celoria 16, I-20133, Milano, Italy*

Internal Report ITeSRE/CNR 273/2000

April 2000

A PRELIMINARY ANALYSIS OF IN-FLIGHT MAIN BEAM RECONSTRUCTION THROUGH EXTERNAL PLANETS FOR PLANCK-LFI

C. Burigana[1], P. Natoli[2], N. Vittorio[2],
N. Mandolesi[1] and M. Bersanelli[3]

[1] *Istituto TeSRE/CNR, via P. Gobetti 101, I-40129 Bologna, Italy*
[2] *Dipartimento di Fisica, Università di Roma "Tor Vergata", via della Ricerca Scientifica 1, I-00133, Roma, Italy*
[3] *Dipartimento di Fisica, Università degli Studi di Milano, via Celoria, I-20131, Milano, Italy*

SUMMARY – In-flight measurements of the shape of the antenna main beams of the Planck instruments is a crucial input to the data analysis pipeline. We study the main beam reconstruction achievable through the observation of external planets using a flight simulator to model the observations of the Solar System bodies. We restrict our analysis to the 30 GHz LFI channel but the method can be easily extended to higher frequency channels. By considering in this preliminary study a bivariate Gaussian beam shape, we show that it is possible to fit the time order data from the external planets (mainly Jupiter and Saturn) to obtain an accurate, simple and fast reconstruction in flight of the main beam parameters independently of the calibration accuracy. We demonstrate that it is possible to combine a very accurate in-flight calibration by using the CMB dipole signature and its modulation introduced by the spacecraft motion and the good accuracy in the recovery of the maximum signal at the planet transit for a measurement of the intrinsic planet temperatures at millimetric wavelengths with an accuracy at % level. This work is based on Planck-LFI activities.

1 Introduction

The Planck Surveyor[1] is the ESA space mission devoted to the study of the Cosmic Microwave Background. Planck will have an impact on a number of scientific issues, such as the physics of the early universe, structure formation theory and cosmological parameters determination (Bersanelli et al. 1996). In order to reach the necessary level of sensitivity it

[1] http://astro.estec.esa.nl/SA-general/Projects/Planck/

is important to understand systematics and to keep them under control. In this work we will focus on the behavior of the PLANCK Low Frequency Instrument (LFI, Mandolesi et al. 1998) antenna patterns. For simplicity, we will restrict our analysis to the 30 GHz LFI channel but the method we present here can be easily extended to higher frequency channels.

The beam pattern is affected by optical distortions, which depend on the telescope design and on the arrangement of the various feed horns in the focal plane. These effects degrade both angular resolution and sensitivity (e.g., Mandolesi et al. 2000a,b). Therefore, accurate measurement of the beam pattern is a crucial input to the data analysis pipeline.

Due to their small angular size external planets produce large signals only when seen in the main beam. As such, they represent a unique possibility to recover directly from the data the in-flight behavior of the main beam. This point was already addressed, in the framework of the PLANCK mission, by Bersanelli et al. 1997 for the simple case of a Gaussian symmetric antenna response. We extend here this analysis to quantify our ability to reconstruct a more realistic, asymmetric beam pattern.

The plan of this work is as follows. In Sect. 2 we describe our main tools and assumptions. In Sect. 3 we discuss the quality of the main beam reconstruction. In Sect. 4 we summarize our findings and draw our conclusions.

2 Method

In order to attack the problem of the in-flight main beam reconstruction, we have to: (*i*) describe the PLANCK orbit and scanning strategy; (*ii*) quantify the antenna response; (*iii*) exploit the planet's mm emission and positions; (*iv*) simulate the PLANCK observations of the external planets (basically Jupiter and Saturn). Here we briefly discuss these points separately.

2.1 PLANCK orbit and scanning strategy

The selected orbit for the PLANCK satellite is a Lissajous orbit around the Lagrangian point L2 of the Sun-Earth system (e.g., Bersanelli et al. 1996). In the nominal operation scheme the spacecraft spins at 1 r.p.m. around an axis kept parallel to the ecliptic plane. Every hour the spin axis is moved by $2.5'$ maintaining its anti-solar direction. The telescope optical axis is at an angle α from the spin axis direction. The spin axis might precede about the anti-solar direction, with a period of about six months and an amplitude of about 10°. This spacecraft movement is of course over imposed to the Lissajous orbit and to the spin axis hourly shift. In this work we consider for simplicity only the case $\alpha = 90^\circ$ with no precessions, but it is evident that the quality of the main beam reconstruction does not depend on the assumed scanning strategy. We make use of the PLANCK flight simulator described in detail by Burigana et al. 1997, 1998 and Maino et al. 1999 properly modified to model the PLANCK observations of the Solar System bodies and the spacecraft motion (see, e.g., Bersanelli et al. 1997).

For what follows, it is convenient to introduce a telescope "reference frame" (hereafter rf) $\{x_T, y_T, z_T\}$ with the z_T axis coincident with the direction of the telescope line of sight (the $\hat{p}$ direction, say) and with the $x_T - y_T$ plane identifying the telescope field of view plane (we choose to orient $\hat{x}_T$ towards the intersection of the $x_T - y_T$ plane with the spin axis $\hat{s}$ or, in the case $\alpha = 90^\circ$, $\hat{x}_T \parallel \hat{s}$). For the considered scanning strategy the spin axis and the telescope directions ($\hat{s}$ and $\hat{p}$, respectively) are easily derived given the observation time, the spinning frequency and the boresight angle α. So it is always possible to pass from a chosen celestial rf to the telescope rf (and viceversa) by a suitable Eulerian rotation of the considered rf.

2.2 Antenna angular pattern

The PLANCK High Frequency Instrument (HFI, Puget et al. 1998) is located at the center of the focal plane. The LFI feed horns surround HFI and are then substantially off-axis. For instance, with a telescope of 1.5 m class, the 30 GHz beams are at about $\simeq 5^\circ$ from $\hat{p}$. So, it is convenient to define a beam rf $\{x_b, y_b, z_b\}$ with the z_b axis coincident with beam axis $\hat{b}$ and with the $x_b - y_b$ plane slightly tilted with respect to the telescope field of view plane (we keep the convention of obtaining the beam rf from the telescope rf through a rotation of the telescope rf about an axis hortogonal to the plane identified by $\hat{p}$ and $\hat{b}$ by the angle necessary to transport $\hat{p}$ to $\hat{b}$).

As we know the position of each feed horn in the focal plane, we can always pass from the telescope rf to the beam rf and viceversa. In fact, the flight simulator determines for every time step the orientations in the sky of the telescope and beam reference frames, to compute the antenna response for a given line of sight.

2.2.1 Main beam

Recent improvements on the PLANCK optical design based on aplanatic solutions (Mandolesi et al. 2000b) show that the main beams are roughly elliptical, with an ellipticity ratio $r \lesssim 1.4$ (Alcatel, private reference, PL-AS-TN-022). Therefore, we approximate the antenna pattern as an off-axis bivariate Gaussian beam. For simplicity, we will consider the bivariate Gaussian beam projected onto the field of view plane (i.e. we will consider this beam representation on the $x_T - y_T$ plane, and not on the $x_b - y_b$ beam plane). To be accurate one has to say that if the true beam shape is elliptical in the $x_b - y_b$ plane, it gets distorted by the projection on the $x_T - y_T$ plane. However, since the off-axis angle even for the 30 GHz beam is small, this distortion is negligible and, if anything, does not change the elliptical nature of the beam response. In addition, a realistic main beam distortion implies a deviation from the elliptical shape larger than that introduced by this projection. So, let (x_T^*, y_T^*) identify the projection of the beam centre unit vector onto the $x_T - y_T$ plane. Let ϵ be the angle between the x_T-axis and the principal axis of the bivariate Gaussian. The (normalized to the maximum) beam response can be then expressed as:

$$J = \exp\left[-\frac{1}{2}\left(\left(\frac{A_+}{\sigma_+}\right)^2 + \left(\frac{A_-}{\sigma_-}\right)^2\right)\right], \qquad (1)$$

where $A_+ = (x_T - x_T^*)\cos\epsilon + (y_T - y_T^*)\sin\epsilon$, $A_- = -(x_T - x_T^*)\sin\epsilon + (y_T - y_T^*)\cos\epsilon$, and σ_+^2 and σ_-^2 are the bivariate's beam dispersions along the ellipse principal axis rotatated by an angle ϵ with respect to the x_T axis in the $x_T - y_T$ plane. It is then convenient to define the beam "sigma" $\sigma = \sqrt{\sigma_+ \sigma_-}$ and the ellipticity ratio $r = \sigma_+/\sigma_-$.

2.3 Planet's mm emissions and positions

Several authors reported measurements of the planets brightness temperature at millimeter wavelengths with typical uncertainties of $3 \div 5\%$ (see, e.g., Bersanelli et al. 1997 and references therein). The quite large uncertainties associated with these values prevents one from using planets for accurate temperature calibration of the PLANCK time order data. This will be done, to better than a 1%, by using the diffuse signature of the CMB dipole anisotropy (Bersanelli et al. 1997). However, for the purpose of beam reconstruction it is not necessary to have a detailed knowledge of the planet emission. It only matters that the source is stable and sufficiently bright to be detectable even when the source is far from the beam axis. This requirement is crucial to sample the antenna beam response at different angles. For this reason we will consider here only Jupiter and Saturn, which are the brightest of the external

planets. On the basis of the published data, we will assume hereafter that Jupiter and Saturn have, at 30 GHz, brightness temperatures of $T^{(b)}_{jup} = 152$ K and $T^{(b)}_{sat} = 133$ K, respectively.

2.4 PLANCK observations of the external planets

We use the PLANCK flight simulator in order to model the transit of the planets in the PLANCK field of view. In particular, Jupiter and Saturn will be observed twice in about a year. The solid angle of the external planets as seen by PLANCK is very small compared to the beam size. Thus, the PLANCK observations of the Jupiter (Saturn) will yield

$$T_{30GHz}[\hat{\gamma}(t)] \simeq \frac{T^{(b)}\pi(R/d)^2 \; J[\hat{\gamma}(t) - \hat{b}]}{\int_{4\pi} J(\hat{\gamma}) \; d\Omega} \, . \tag{2}$$

In this equation T_{30GHz} is the observed Jupiter (Saturn) brightness temperatures @ 30 GHz; $T^{(b)}$, R and d represent the intrinsic Jupiter (Saturn) brightness temperature, radius and distance, respectively; J is the antenna response and $\hat{\gamma}(t)$ identifies the angular position of the planet as seen by PLANCK, the time dependence being fixed by the scanning strategy.

3 In-flight recovery of the main beam pattern

The PLANCK Time Ordered Data (TOD) are affected by instrumental noise. Therefore, our capability to recover the main beam pattern rests on the possibility to clearly detect a bright source (e.g., Jupiter), even when significantly far from the beam axis. A proper description of the PLANCK-LFI instrumental noise should in principle include a $1/f$ contribution (see, e.g., Bersanelli et al. 1996, Seiffert et al. 1997). The knee-frequency of the $1/f$ noise is expected to be comparable with the spinning frequency. However, it has been shown that destriping algorithms can very efficiently remove this low frequency noise component even under more pessimistic conditions (see, e.g., Maino et al. 1999 and references therein) and return a TOD that we will assume, accordingly with the goals of this work, white noise dominated. So, in what follows we will model the TOD noise component as pure white noise, with the PLANCK goal sensitivities discussed by Bersanelli et al. 1999 (private reference, PLANCK Low Frequency Instrument, Instrument Science Verification Review, October 1999, LFI Design Report). In principle, the signal fluctuations introduced by CMB and foreground anisotropies behave as a noise source in this context. However, since they can be accurately subtracted from the TOD by using the PLANCK final maps, we neglect them in what follows. In the simulations presented in Sect. 3.1, we oversample each scan circle every $\simeq 5'$ (i.e. roughly 6 points per FWHM @ $30GHz$) and shift the spin axis by $5'$ every two hours. After simulating the Jupiter and Saturn transits we extract from the time ordered scans a few (~ 100) chunks comprising the source transit. Since the source is pointlike, these chunks give, when displayed one after the other and having taken into account the small variations of planet distance in the different samplings, a 2-D plot of the beam profile, $\simeq 8.3^\circ \times 8.3^\circ$ wide.

In Fig. 1 we show the expected signal from Jupiter as seen along the scan circle which crosses the source at the maximum (top panel) and as seen along an arc orthogonal to this circle (bottom panel). The signal to noise can be improved, wrt the case of a single receiver and transit, by considering that two LFI receivers are coupled to the same optical beam, that there are two 30 GHz beams with the same optical properties and that two (three) transits of both Jupiter and Saturn are expected for a one year (for a $14 \div 15$ months) mission. This obviously increases the signal to noise ratio by a factor of $2\sqrt{2}$ ($2\sqrt{3}$). As a result, @ 30

GHz, the shape of the main beam can be recovered down to $-(25 \div 32.5)$ dB, i.e. at about $(3.5 \div 4)\sigma$.

3.1 Recovery of the main beam parameters

We consider both a symmetric and an elliptical beam, with ellipticity ratio $r = 1.3$. The numerical values of the beam parameters are shown in Table 1. We use Eq.(1) to model the antenna response. We fit the beam shape theoretical parameters to the 2D plot of the beam response obtained as mentioned at the end of the previous section.

The results of the fits are shown in Table 2. We fit also an additional parameter, r_k, related to the planet brightness temperature and to the average distance of the planet from the spacecraft, $\langle d \rangle$, for the points considered in the fit: $r_k = \pi(R/\langle d \rangle)^2 T^{(b)} / \int_{4\pi} J(\hat{\gamma})\, d\Omega$. We recover the full set of parameters with very high accuracy, the $\chi^2/\,\mathrm{DOF}$ being always very close (to better than 1%) to the unity value. It is obviously more efficient to recover the beam pattern parameters using Jupiter rather than Saturn, simply because Jupiter is brighter.

An interesting byproduct of the beam fitting procedure is the possibility of estimating the planet's antenna temperature, or more properly the product $T^{(b)}R^2$ relevant for the planet's emission at the considered frequency. This quantity, as previously stated, is a poorly known quantity at LFI's frequencies. By considering Eq. (2) it is clear that the latter temperature, $T^{(b)}$ is related to the normalization of the bivariate which is in turn very well constrained by our fit. The ability to estimate $T^{(b)}$ then rests upon the overall calibration accuracy[2] and on the knowledge of the total antenna beam integral. Calibration for PLANCK will be provided by continuous observation of the CMB dipole signature and its modulation introduced by the spacecraft motion (Bersanelli et al. 1997) and is expected to be accurate to within 1%. The total integral of the antenna pattern poses a more serious problem, as the contribution of the far side lobes goes undetected when using a celestial source. However, optical calculations (de Maagt 1998) show that the contribution to the antenna pattern coming from outside the main lobe is expected to be $< (2 \div 3)\%$ of the total. The uncertainty on the latter figure may then dominate and pratically set the accuracy on the LFI estimate of $T^{(b)}$; therefore, even a poor knowledge of this contribution (e.g., with an accuracy of $\sim 30\%$) allow to reach a $\simeq 1\%$ level of accuracy in the measurement of $T^{(b)}$.

4 Discussion and conclusions

We implemented the PLANCK flight simulator (Burigana et al. 1997, 1998, Maino et al. 1999) to properly discuss the impact of the Solar System main bodies on the PLANCK observations. In particular, we focused on the problem of the in-flight reconstruction of the main beam of the PLANCK-LFI antenna patterns. To do so, we simulate in details the transits of Jupiter and Saturn in the field of view of the PLANCK-LFI, 30 GHz beam. The method can be easily extended to the other PLANCK channels. Our analysis shows that, using Jupiter, we can recover in flight the main beam response down to $\sim -(25 \div 32.5)$ dB, where the signal to noise ratio approaches unity.

Both circular and elliptical Gaussian beams have been considered, but the method can be generalized to more refined parametrizations.

We have demonstrated that the key parameters of the main beam (resolution, ellipticity, position and inclination on the plane of PLANCK field of view) can be simultaneously recovered with high precision by fitting the planet transit signal. Of course, the larger signal to noise

[2]We want to stress that the calibration of the TOD is not needed in order to reconstruct the other beam parameters.

ratio of Jupiter (compared to that of Saturn) translates in a better parameter recovery, by a factor $3 \div 5$.

The possibility to combine a very accurate in-flight calibration by using the CMB dipole (Bersanelli et al. 1997) and the good accuracy in the recovery of the maximum signal (the parameter r_k in Table 2) at the planet transit, offers a good chance of measuring the intrinsic planet temperatures at millimetric wavelengths with an accuracy at % level, the main source of error being the uncertainty on the integrated antenna pattern response. This represents an interesting byproduct of PLANCK observations.

To summarize, at least at 30 GHz, observation of external planets offers an accurate and simple method to reconstruct in flight the main beam parameters under very general conditions.

In the future we want to extend the analysis to more realistic main beam shapes, like those computed by optical simulation codes, and take into account the effects introduced by the spacecraft pointing uncertainty and the beam smearing due to the satellite rotation.

Acknowledgements. It is a pleasure to thank C.R. Butler, B. Cappellini, G. Cremonese, D. Maino, F. Pasian and F. Villa for useful discussions on PLANCK design and performances and on planet emission properties.

References

[1] Bersanelli M. et al., 1996, ESA, COBRAS/SAMBA Report on the Phase A Study, D/SCI(96)3

[2] Bersanelli M. et al., 1997, A&AS, 121, 393

[3] Burigana C. et al., 1997, Int. Rep. TeSRE/CNR 198/1997

[4] Burigana C. et al., 1998, A&AS, 130, 551

[5] Burigana C., et al., 2000, Astro. Lett. Comm., in press, astro-ph/9903137

[6] De Maagt P., Polegre A.M. & Crone G., 1998, PLANCK – Straylight Evaluation of the Carrier Configuration, Technical Report ESA, PT-TN-05967, 1/0

[7] Maino D. et al., 1999, A&AS, 140, 1

[8] Mandolesi N. et al., 1998, PLANCK Low Frequency Instrument, A Proposal Submitted to the ESA

[9] Mandolesi N., et al., 2000a, A&AS, in press

[10] Mandolesi N., et al., 2000b, Astro. Lett. Comm., in press, astro-ph/9904135

[11] Puget, J.L. et al., 1998, High Frequency Instrument for the PLANCK Mission, A Proposal Submitted to the ESA

[12] Seiffert M., et al., 1997, Rev. Sci. Instrum., submitted

Figure 1: Top panel: signals of different components along the scan circle with the maximum of Jupiter contribution during its first transit. Solid line: Jupiter signal; crosses: white noise; diamonds: $1/f$ noise coupled to white noise; dotted line: signal from CMB and extragalactic source fluctuations and Galaxy emission modelled according to Burigana et al. 2000 and references therein. Bottom panel: the same as in the top panel, but considering the signal at the same scan position, where Jupiter signal is maximum, for different scan circles. According to the simulation parameters, by multiplying the scan circle number or the sampling number on the scan circle by 5 we have respectively the angular displacement between different scan circles and (approximately, owing to the off-axis beam position) the angular displacement between different samplings along the scan circle, expressed in arcmin. We consider here the case of an elliptical beam with $r = 1.3$, clearly visible in the different spread of Jupiter signal in the two panels. Note that the signal to noise ratio is larger than unit up to $-(20 \div 25)$ dB, i.e. at about $(3 \div 3.5)\sigma$. [Signals in dB normalized to the maximum Jupiter signal at its first transit].

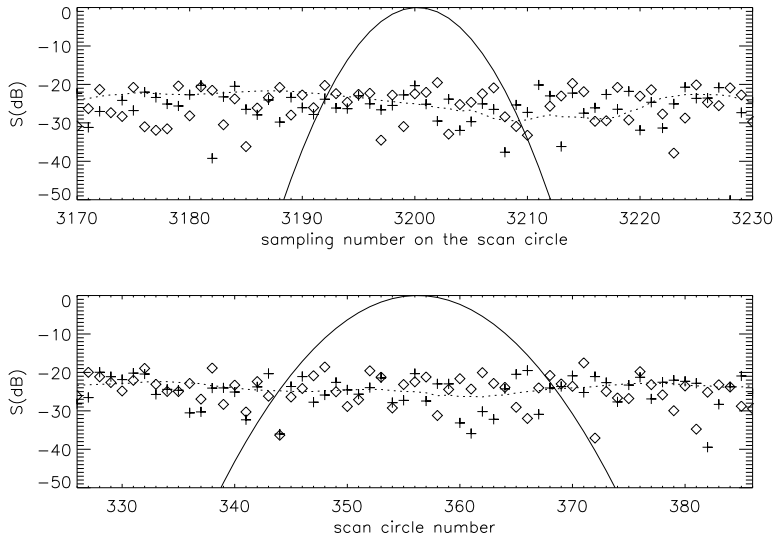

Table 1: Input parameters of symmetric and elliptical beam for the considered planet transits.

Input values								
Event	ϵ (deg)		σ (arcmin)	r –		r_k ‡ (mK)	$x_T^* \cdot 10^2$ –	$y_T^* \cdot 10^2$ –
	circ.	*ellipt.*		*circ.*	*ellipt.*			
Jupiter (I)	–	0	14.01381	1	1.3	35.8297	−5.76035	7.91971
Jupiter (II)						35.4743		
Saturn (I)						7.8543		
Saturn (II)						7.8229		

‡ The value r_k depends on the distance between the spacecraft and the planet which slightly varies between different pointing events.

Table 2: Recovery of the beam parameters from the considered planet transits.

Event	ϵ (deg)	σ (arcmin)	r –	r_k (mK)	$x_T^* \cdot 10^2$ –	$y_T^* \cdot 10^2$ –	$\chi^2/\,\mathrm{DOF}$ –
Circular beam							
Jupiter (I)	–	14.0071 ±0.0089	1.0039 ±0.0012	35.877 ±0.032	−5.7602 ±0.0004	7.9192 ±0.0004	0.994
Jupiter (II)	–	14.0126 ±0.0092	1.0010 ±0.0013	35.486 ±0.033	−5.7603 ±0.0004	7.9200 ±0.0004	0.997
Saturn (I)	–	13.996 ±0.042	1.0067 ±0.0061	7.839 ±0.033	−5.7659 ±0.0020	7.9204 ±0.0015	0.998
Saturn (II)	–	14.034 ±0.042	1.0078 ±0.0061	7.797 ±0.033	−5.7637 ±0.0020	7.9209 ±0.0015	1.007
Elliptical beam							
Jupiter (I)	−0.0059 ±0.0024	14.0095 ±0.0088	1.3023 ±0.0016	35.876 ±0.032	−5.7602 ±0.0004	7.9193 ±0.0003	0.995
Jupiter (II)	0.0011 ±0.0025	14.0102 ±0.0092	1.2993 ±0.0017	35.491 ±0.033	−5.7603 ±0.0004	7.9199 ±0.0003	0.997
Saturn (I)	−0.007 ±0.011	14.004 ±0.042	1.3055 ±0.0078	7.837 ±0.033	−5.7661 ±0.0020	7.9199 ±0.0015	0.999
Saturn (II)	0.009 ±0.011	14.041 ±0.042	1.3073 ±0.0078	7.796 ±0.033	−5.7645 ±0.0020	7.9207 ±0.0015	1.007